

Algorithm and System Co-design for Efficient Subgraph-based Graph Representation Learning

Haoteng Yin[†], Muhan Zhang[‡], Yanbang Wang[§], Jianguo Wang[†], Pan Li[†]

[†]Department of Computer Science, Purdue University [‡] Institute for Artificial Intelligence, Peking University

[§]Department of Computer Science, Cornell University

[†]{yinht, csjgwang, panli}@purdue.edu [‡] muhan@pku.edu.cn [§] ywangdr@cs.cornell.edu

ABSTRACT

Subgraph-based graph representation learning (SGRL) has been recently proposed to deal with some fundamental challenges encountered by canonical graph neural networks (GNNs), and has demonstrated advantages in many important data science applications such as link, relation and motif prediction. However, current SGRL approaches suffer from a scalability issue since they require extracting subgraphs for each training and testing query. Recent solutions that scale up canonical GNNs may not apply to SGRL. Here, we propose a novel framework SUREL for scalable SGRL by co-designing the learning algorithm and its system support. SUREL adopts walk-based decomposition of subgraphs and reuses the walks to form subgraphs, which substantially reduces the redundancy of subgraph extraction and supports parallel computation. Experiments over seven homogeneous, heterogeneous and higher-order graphs with millions of nodes and edges demonstrate the effectiveness and scalability of SUREL. In particular, compared to SGRL baselines, SUREL achieves 10× speed-up with comparable or even better prediction performance; while compared to canonical GNNs, SUREL achieves 50% prediction accuracy improvement. SUREL is also applied to the brain vessel prediction task. SUREL significantly outperforms the state-of-the-art baseline in both prediction accuracy and efficiency.

XXXXX Reference Format:

Haoteng Yin[†], Muhan Zhang[‡], Yanbang Wang[§], Jianguo Wang[†], Pan Li[†]. Algorithm and System Co-design for Efficient Subgraph-based Graph Representation Learning. PVLDB, 14(1): XXX-XXX, 2020.
doi:XX.XX/XXX.XX

PVLDB Artifact Availability:

The source code, data, and/or other artifacts have been made available at <https://github.com/Graph-COM/SUREL.git>.

1 INTRODUCTION

Graph-structured data is prevalent to model relations and interactions between elements in real-world applications [21]. Graph representation learning (GRL) aims to learn representations of graph-structured data and has recently become a hot research topic [14].

Previous works on GRL focus on either model design or system design while very few works jointly consider them. Works on model design tend to propose more expressive, generalizable and robust GRL models while paying less attention to their deployment [29, 41]. Hence, many theoretically powerful models can hardly apply to real-world large graphs. On the other hand, research on system design focuses on system-level techniques for better model development, such as graph partitioning [8], sub-sampling [15, 52] and pipelining [19, 38, 53, 57]. However, they only consider basic GRL models, in particular the standard graph neural network (GNN) models, yet often ignore their modeling limitations to solve practical GRL tasks.

Canonical GNNs [15, 20] share a common framework: each node is associated with a vector representation that gets iteratively updated by aggregating the representations from its neighboring nodes via graph convolution layers. The final prediction is made by combining the representations of nodes of interest. Although recent successes in system research have greatly pumped up the efficiency [11, 43], the GNN framework intrinsically suffers from three modeling limitations. First, one single node representation may over-squash the information that is potentially useful for multiple downstream tasks [9]. When multiple tasks associated with one node are requested, e.g., to predict multiple relations or links attached to this node, single node representation alone yields sub-par performance. Second, intra-node distance information cannot be captured by canonical GNNs due to the limited GNN expressive power [22], which leads to the failure of GNNs in the prediction tasks over a set of nodes (See Fig. 1a), such as substructure counting [4, 7] and higher-order pattern prediction [34, 56]. Third, the depth of a GNN is entangled with the range of the receptive field. So, using a deeper GNN to impose more non-linearity has to include a larger but perhaps unnecessary receptive field, which risks contaminating the representations with irrelevant information [17, 51]. We leave more detailed explanations in Supp. B.

Therefore, subgraph-based GRL (SGRL) recently has emerged as a new trend and has shown superior performance in many data science tasks such as, node structural role prediction [22], link prediction [22, 54, 56], relation prediction [37], higher-order pattern prediction [22, 26], temporal network modeling [45], recommender system design [55], graph meta-learning [17], and subgraph matching [25, 27] and prediction [44]. Different from the canonical GNNs, SGRL extracts a local subgraph patch for each training and testing query and learns the representation of the subgraph patch to make the final prediction (See Fig. 1b). For example, SEAL [54, 56] learns the representation of a subgraph around a node pair to predict the link between the node pair. This framework fundamentally overcomes the above three limitations. First, subgraph extraction

This work is licensed under the Creative Commons BY-NC-ND 4.0 International License. Visit <https://creativecommons.org/licenses/by-nc-nd/4.0/> to view a copy of this license. For any use beyond those covered by this license, obtain permission by emailing info@vldb.org. Copyright is held by the owner/author(s). Publication rights licensed to the VLDB Endowment.

Proceedings of the VLDB Endowment, Vol. 14, No. 1 ISSN 2150-8097.
doi:XX.XX/XXX.XX

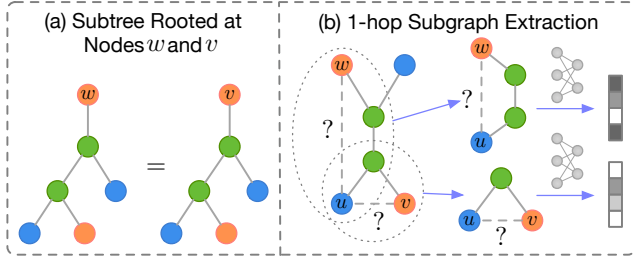


Figure 1: A Toy Example of SGRL: the task is to predict whether uw or uv is more likely to form a link. Ideally, if this comes from a social network, uv is more likely linked because they share a common neighbor. However, canonical GNNs cannot tell such difference since w and v share the same subtree structures so that it gives those two nodes the same representation [47]. SGRL solves this problem by extracting the subgraph patches around each queried node pair. Prediction based on the subgraph representation provides much better performance than canonical GNNs [54].

allows decoupling the contributions made by a node to different queries, which naturally prevents over-squashing the information. Second, subgraph patches can be paired with intra-node distance features much more easily than working the full graph, where the distance features are known to be crucial for the prediction over a set of nodes [22]. Third, subgraph extraction disentangles the model depth and the range of receptive field, which allows learning a rather non-linear model with only relevant local subgraphs as the input.

Despite the importance, the SGRL framework has not received as much attention as the canonical GNN framework in the system research community. The potential challenge comes from the subgraph extraction step of SGRL, which could be rather irregular and time consuming. Specifically, SGRL requires to materialize a subgraph patch for each sample during training and inference. Previous works for SGRL extract subgraphs for all training and testing queries offline [26, 54]. However, offline subgraph extraction is not scalable for large graphs due to the huge memory consumption. Online subgraph extraction [51], on the other hand, takes a great amount of processing time, as the irregularity of subgraphs makes the extraction procedure hard to be efficiently parallelized.

Here, we aim to fill the gap by designing a novel computational framework SUREL, to support SGRL over large graphs. SUREL consists of a new system-friendly learning algorithm for SGRL and a scalable system to support this algorithm. We do not develop a system to directly support the current SGRL approaches, since the bottleneck induced by the subgraph extraction of all current SGRL approaches is hard to be overcome. One crucial design of SUREL is to avoid the overhead caused by the online subgraph extraction.

The key idea behind SUREL is to break (and down-sample) subgraphs into random walks which have regular sizes, that can be easily sampled, and more importantly, can be reused among different subgraphs. To compensate for the loss of structural information after subgraph decomposition, we propose to use relative positional encoding (RPE), an intra-node distance feature that records the position of each node in the subgraph. Specifically, for every node u in the network, during preprocessing, SUREL samples and records

a certain number of random walks that start from u . Meanwhile, SUREL counts the step occurrence of each node in the walks as its RPE vector. The set of walks paired with RPEs can be viewed as a subgraph patch centered at u . The number and the length of those random walks are small constants for every node, thus the memory and time consumption here only linearly depend on the number of nodes. Moreover, such preprocessing can be done in parallel and offline. For training and inference, given a queried node set Q , SUREL first groups the sampled walks originated from the nodes in Q . Then, it implicitly joins the subgraphs centered at each node in Q by joining the RPEs into a query-level RPE for all the associated nodes, which can be executed in full parallel. Finally, SUREL uses neural networks to learn the representation of the grouped set of these walks to make the final prediction. As these walks are regular, the learning procedure can be done fast by GPUs. We also design a dedicated query mini-batching pipeline to further improve the data reuse. The system architecture of SUREL is illustrated in Fig. 2.

Our contributions can be summarized as follows:

- **A Novel System-Friendly Algorithm.** We propose the first scalable algorithm for SGRL tasks by adopting a novel walk-based computation framework. This framework uses regular data structures and allows extreme system acceleration.
- **Dedicated System Support (Open-source).** We design SUREL to support the proposed algorithm. It can rapidly sample and join walk features to represent multiple subgraphs in parallel. SUREL adopts many system optimization techniques including parallelization, memory management, load balancing, etc.
- **High Performance and Efficiency.** We evaluate SUREL over link/relation/motif three prediction tasks over 7 real-world graphs of millions of nodes/edges. SUREL significantly outperform the current SGRL approaches, and executes 10× faster in training and testing. Meanwhile, benefiting from the SGRL essence, SUREL outperforms canonical GNNs by a great margin on prediction performance (almost 50% in all tasks).

2 PRELIMINARIES AND RELATED WORKS

In this section, we set up notations, formulate the SGRL problem and review some related works. Frequently used symbols are summarized in Table 1 for quick reference.

2.1 Notations

Definition 2.1 (Graph-structured data). Let $\mathcal{G} = (\mathcal{V}, \mathcal{E}, X)$ denote an attributed graph, where $\mathcal{V} = [n] = \{1, 2, \dots, n\}$ and $\mathcal{E} \subseteq \mathcal{V} \times \mathcal{V}$ are the node set and the edge set respectively. $X \in \mathbb{R}^{n \times d}$ denotes the node attributes with d -dimension. Further, we use \mathcal{N}_v to represent the set of nodes in the direct neighborhood of node v , i.e., $\mathcal{N}_v = \{u : (u, v) \in \mathcal{E}\}$.

Definition 2.2 (m -hop Subgraph). Given a graph \mathcal{G} and a node set of interest Q , let \mathcal{G}_Q^m denote the m -hop neighboring subgraph w.r.t the set Q . \mathcal{G}_Q^m is the induced subgraph of \mathcal{G} , of which the node set \mathcal{V}_Q^m includes the set Q and all the nodes in \mathcal{G} whose shortest path distance to Q is less than or equal to m . Its edge set is a subset of \mathcal{E} , where each edge has both endpoints in its node set \mathcal{V}_Q^m . The nodes in \mathcal{V}_Q^m still carry the original node attributes if \mathcal{G} is attributed.

Table 1: Summary of Frequently Used Notations.

Symbol	Meaning
Q	a query (set of nodes), i.e. $Q = \{u, v, w\}$
\mathcal{Q}	a collection of queries, i.e. $Q \in \mathcal{Q}$
\mathcal{W}_u	the set of walks starting from node u
\mathcal{W}	a collection of walks, i.e. $W \in \mathcal{W}$
\mathcal{V}_u	set of unique nodes appeared in \mathcal{W}_u
\mathcal{X}_u	the relative positional encoding (RPEs) of nodes in \mathcal{V}_u regarding their step occurrence in \mathcal{W}_u
$\mathcal{X}_{u,v}$	the RPE vector of node v regarding the node u (all zeros if $v \notin \mathcal{V}_u$)
\mathcal{T}	the RPE array with indices as RPE-IDs and entries as RPE vector
\mathcal{H}_u	the dictionary with nodes in \mathcal{V}_u as keys and RPEs \mathcal{X}_u (or RPE-IDs) as values
\mathcal{A}	the associative array with nodes in $u \in \mathcal{V}$ as key and the tuple $(\mathcal{W}_u, \mathcal{X}_u)$ as entry
\uplus	the concatenation operation that joining all RPEs, i.e. join $\mathcal{X}_{u,x}$ for $u \in Q$ as $[\dots, \mathcal{X}_{u,x}, \dots]$.
$\mathcal{X}_{Q,x}$	the query-level RPE for node x , $\mathcal{X}_{Q,x} = \uplus_{u \in Q} \mathcal{X}_{u,x}$

2.2 Graph Learning Problems and Background

Now, we formally formulate the GRL and SGRL problems.

Definition 2.3 (Graph Representation Learning (GRL)). Given a graph \mathcal{G} and a queried set of nodes Q , graph representation learning aims to learn a mapping from the graph-structured data to some predicting labels as $f(\mathcal{G}, Q) \rightarrow y$, where the mapping $f(\mathcal{G}, Q)$ may reflect structures and node attributes of \mathcal{G} and their relation to Q .

Next, we define SGRL where for a particular query Q , the predictions are made based on the local subgraph around Q .

Definition 2.4 (Subgraph-based GRL (SGRL)). Given a node set Q over an ambient graph \mathcal{G} and a positive integer m , SGRL is to learn the mapping to some labels, which takes the m -hop neighboring subgraph of Q in G as the input $f(G_Q^m, Q) \rightarrow y$. An SGRL task typically is given some labeled node set queries $\{(Q_i, y_i)\}_{i=1}^L$ for training and other unlabeled node set queries $\{Q_i\}_{i=L+1}^{L+N}$ for testing.

We list a few important examples of SGRL tasks. **Link prediction** seeks to estimate the likelihood of a link between two endpoints in a given graph. Additionally, it can be generalized to predict the type of link, such as relation prediction for heterogeneous graphs. In this case, the set Q corresponds to a pair of nodes. Previous studies on network science have identified the importance of leveraging the local induced subgraphs for link prediction [23]. For example, the number of common friends (shown as neighbors in a social network) implies how likely two individuals may become friends in the future. Hence, local subgraphs provide crucial features. The following prediction task for higher-order pattern can be viewed a generalization of link prediction. For **higher-order pattern prediction**, the set Q consists of three or more nodes. The goal is to predict whether the set of nodes in Q will eventually foster a covered edge (termed hyperedge).

Graph neural networks (GNNs). Canonical GNNs associate each node v with a vector representation \mathbf{h} , which is learned and updated by aggregating messages from v 's neighbors, as

$$\mathbf{h}_v^k = \text{UPDATE} \left(\mathbf{h}_v^{k-1}, \text{AGGREGATE} \left(\{\mathbf{h}_u^{k-1} | u \in \mathcal{N}_v\} \right) \right).$$

Here, UPDATE is implemented by neural networks while AGGREGATE is a pooling operation invariant to the order of the neighbors. By unfolding the neighborhood around each node, the computation graph to get each node representation forms a tree structure.

According to Def. 2.4, canonical GNNs seem also able to perform SGRL by encoding the local subtree rooted at each node into the node representation (Fig. 1a). However, in this way, each node representation actually reflects the subgraph around the node **separately** and cannot **jointly** represent the subgraph around multiple nodes, which yields the problem in Fig. 1. However, the SGRL framework considered in this work is able to learn the joint subgraph around a queried node set.

2.3 Other Related Works

Although previous works without exception focus on improving the scalability of canonical GNNs and their system support, some of their techniques inspire the design of SUREL.

To overcome the memory bottleneck of GPU when processing large-scaled graphs, sub-sampling the graph structure is a widely adopted strategy. GraphSAGE [15] and VR-GCN [6] use uniform sampling schema and variance reduction technique respectively to restrict the size of node neighbors; PIN-SAGE [49] exploits Personalized PageRank (PPR) scores to sample neighbors. FastGCN [5] and ASGCN [18] perform independent layer-wise node sampling to allow neighborhood sharing. Cluster-GCN [8] and GraphSAINT [52] study subgraph-based mini-batching approaches to reduce the training graph sizes. Note that the subgraphs in our setting are substantially different from theirs, since our subgraphs work as features for queries while their subgraphs are a compensatory choice to achieve better scalability.

Many works better the system support for GNNs. DGL [43] and PyG [11] are designed for scalable single-machine GNN training. AliGraph [48] develops a distributed system that addresses the storage issue when applying GNNs to massive industrial graphs. AGL [53] is a subgraph-based distributed system for GRL. ROC [19] is a distributed multi-GPU framework for deeper and larger GNN models. Through computation separation and serverless computing, Dorylus offers a CPU-based distributed system for GNN training [38]. G³ speedups GNN training via supporting parallel graph-structured operations [24]. Zhou et al. [58] uses feature dimension pruning to accelerate large-scale GNN inference. However, all these systems only support canonical GNNs so that they all suffer from the intrinsic modeling limitations of GNNs.

3 THE ARCHITECTURE OF SUREL

In this section, we first give an overview of the SUREL framework as shown in Fig. 2. Then, we focus on the design and the implementation of the three modules: Walk Sampler & Relative Position Encoder (Preprocessing), Walk-based Subgraph Storage, Query-based Subgraph Joining & Neural Encoding. At last, we elaborate the efficient training pipeline with Subgraph Query Mini-batching.

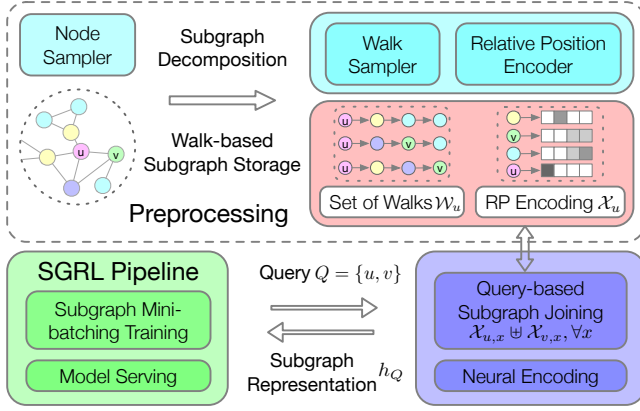


Figure 2: The System Architecture of Subgraph-based Graph Representation Learning Framework (SUREL).

3.1 Overview

Existing SGRL frameworks that extract a subgraph per query do not support efficient training and inference. m -hop subgraph extraction faces the size “explosion” issue as many nodes have significantly large degrees in real-world networks. Moreover, the varying sizes of subgraphs result in fluctuated workload, yielding difficulties in load balancing and memory management.

Compared to subgraph extraction, walk-based downsampling approaches naturally sidestep subgraph size problems through regulating the number and the length of the sampled walks. For every node in the graph, SUREL reduces the subgraph around it by sampling a set of walks originated from the node during preprocessing. To compensate for the information loss by breaking subgraphs into walks, an intra-node distance feature termed relative positional encoding (RPE) is proposed, which enables locating each sampled node in the subgraph. The sampled set of walks paired with RPEs are then recorded into the walk-based subgraph storage through a dedicated data structure, which is designed to support fast and intensive access.

For training and testing, given a query (set of nodes), SUREL employs *subgraph joining* to implicitly construct the subgraph around the entire query, which gets done in a fully parallel fashion. Firstly, all the walks originated from the queried node set are grouped, and then the previous node-level RPEs are joined into a query-level RPE. SUREL further adopts neural networks to encode the walks paired with RPE and makes the final prediction based on the obtained subgraph representation. We also design a mini-batching strategy for training, by leveraging query overlaps to maximize data reuse.

3.2 Preprocessing - Walk Sampling & Encoding

The bottleneck of current SGRL frameworks is how to rapidly acquire the m -hop neighbors for each queried set of nodes, which is a disposable procedure with inherent dependency. SUREL proposes to decompose the m -hop subgraph into a set of m -length walks over the graph that start from each node in the queried set of nodes. Each set contains M walks. This yields several benefits. First, walks are regular and thus extremely efficient to be stored and accessed. Secondly, sub-sampling subgraphs by walks intrinsically addresses the

computational issues induced by the long-tail node degree distribution. Most importantly, the sampled walks grouped with respect to their starting nodes can be potentially shared by different subgraph queries. Our design decouples SGRL from redundant subgraph extraction and empowers the reusability of pre-processed data. We summarize the routine of pre-processing in SUREL coupling with the support of hash-indexed storage in Algorithm 1 and introduce the specifics next.

Walk Sampling. During preprocessing, SUREL samples M -many m -step walks for every node in the given graph. As Fig. 3 (upper left) shows, the sampled walks are grouped in a set \mathcal{W}_u , where u denotes the starting node of walks. The job of walk sampling can be easily divided into parallelizable pieces. We implement the parallelization based on NumPy and OpenMP framework in C. Moreover, to further accelerate walk sampling, we use compressed sparse row (CSR) to represent the graph. The CSR format consists of two arrays, `idxptr` of length $|\mathcal{V}| + 1$ used to record the degrees of nodes, and `indices` of size $|\mathcal{E}|$, each row of which corresponds to the neighbor list per node. CSR allows intensive fast access to the neighbors of a node while maintaining low memory consumption of the graph, which is vital for walk sampling in large-scale graphs.

Relative Positional Encoding (RPE). Structural information gets lost by decomposing subgraphs into walks. SUREL compensates such loss via RPE to locate the relative position of a node in each subgraph, which characterizes the structural contribution of the node to its corresponding subgraph.

For each set of walks \mathcal{W}_u , we first establish a set \mathcal{V}_u that contains distinct nodes appearing in walks of \mathcal{W}_u . Define RPE $\mathcal{X}_u : \mathcal{V}_u \rightarrow \mathbb{R}^{m+1}$ as follows: for each node $x \in \mathcal{V}_u$, a vector $\mathcal{X}_{u,x} \in \mathbb{R}^{m+1}$ is assigned, where $\mathcal{X}_{u,x}[i]$ is the frequency of node x appearing at position i in all walks of \mathcal{W}_u . In SUREL, RPE can be computed on the fly as walks get sampled, thus resulting in nearly zero extra computational cost. The set of walks \mathcal{W}_u paired with the RPE \mathcal{X}_u essentially characterize a sub-sampled subgraph around the node u . Next, we present a dedicated data structure to host \mathcal{W}_u and \mathcal{X}_u .

3.3 Walk-based Subgraph Storage

It is easy to manage the sampled set of walks due to its regularity. An $M * m$ -sized chunk is allocated to each set of walks, which assists to speed up the data fetching. The challenge comes from the management of RPE \mathcal{X}_u , because its size $|\mathcal{V}_u|$ varies across different target nodes. One naïve way to handle such irregularity is to directly attach the RPE $\mathcal{X}_{u,x}$ to each node x in the walks of \mathcal{W}_u . However, this gives an $M * m * (m + 1)$ tensor that consumes huge amount of memory. Moreover, it loses the track of node indices that are used to join subgraphs later.

We design a data structure (see Fig. 3) by using an associative array \mathcal{A} indexed by each $u \in \mathcal{V}$, with the tuple $(\mathcal{W}_u, \mathcal{H}_u)$ as the corresponding entry, where \mathcal{W}_u is a set of walks and \mathcal{H}_u is a dictionary. An array \mathcal{T} is introduced to record the values of RPEs. The dictionary \mathcal{H}_u maps the key $x \in \mathcal{V}_u$ to an integer RPE-ID $_{u,x}$, which is the index of RPE $\mathcal{X}_{u,x}$ in \mathcal{T} . This design guarantees the access of RPE in $O(1)$ time.

The above \mathcal{A} and \mathcal{H}_u are built on top of uthash’s C macros¹, with additional support of arbitrary insertions and deletions of

¹<https://troydhanon.github.io/uthash/>

Algorithm 1: Data Preprocessing in SUREL

Input: Graph \mathcal{G} ; number of walks M ; step of walks m

Output: Associative array \mathcal{A} , RPE array \mathcal{T}

- 1 Initialize the array \mathcal{A} and \mathcal{T} , the dictionary \mathcal{H}
 - 2 **for** each node $u \in \mathcal{G}$ **do**
 - 3 Run M times m -step random walks on \mathcal{G} as a set of walk $\mathcal{W}_u \in \mathbb{Z}^{M \times m}$;
 - 4 Add the key $\mathcal{V}_u = \text{set}(\mathcal{W}_u)$ to \mathcal{H}_u ;
 - 5 Calculate RPE for $x \in \mathcal{V}_u$, save its values $\mathcal{X}_{u,x}$ to \mathcal{T} , and write the index RPE-ID $_{u,x}$ in \mathcal{T} back to $\mathcal{H}_u(x)$;
 - 6 Insert $\{u : (\mathcal{W}_u, \mathcal{H}_u)\}$ to \mathcal{A}
 - 7 **end**
 - 8 Pruning \mathcal{T} and update the value of \mathcal{H} by re-indexing.
-

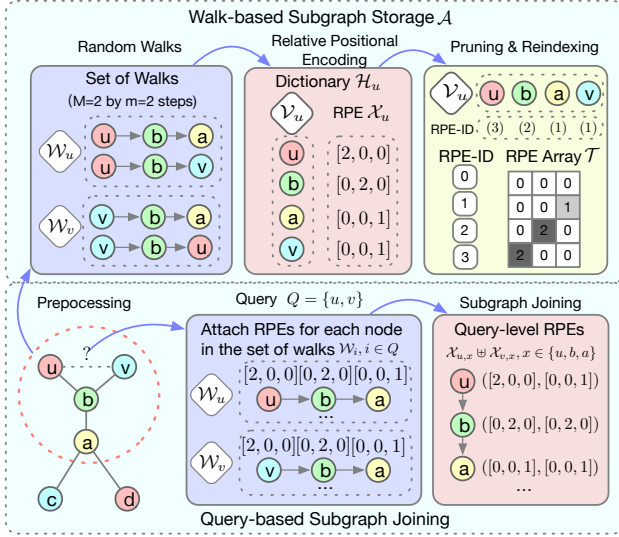


Figure 3: An Illustration of Joining RPE into Query-level RPEs with the Support of Walk-based Subgraph Storage.

key-value pairs into the dictionary. It offers data access and search in $O(1)$ time on average, which is approximately as good as the direct address table but greatly reduces the space wastage. Particularly, it has no dependency or need for communication between multiple hash queries, thus can be pleasingly executed in parallel. Both \mathcal{A} and \mathcal{H}_u are stored in RAM on the CPU side.

The array \mathcal{T} is trimmed to remove duplicates once all set of walks get sampled (and thus all RPE \mathcal{X}_u 's get determined). The shape of \mathcal{T} is regular and its size is small in practice, thus it can be hosted in the GPU. We find it is crucial to pin RPEs in GPU memory since it can significantly reduce the communication cost of moving data back and forth between the RAM and GRAM.

3.4 Query-based Subgraph Joining

The storage designed above records the downsampled subgraph around each node. As SGRL is mostly useful for making predictions

over a set of nodes Q , here we further illustrate how to get the joined subgraph around all the nodes $u \in Q$.

The idea is to concatenate all set of walks $[\dots, \mathcal{W}_u, \dots]$ for $u \in Q$, since each set of walks \mathcal{W}_u can be viewed as a subgraph around u . Besides, each node x in the walks will be paired with a *query-level* RPE $\mathcal{X}_{Q,x}$ that characterizes the relative position of node x in the joint subgraph around the nodes in Q . Specifically, $\mathcal{X}_{Q,x}$ is defined by joining all RPEs $\mathcal{X}_{u,x}$ for $u \in Q$, i.e., $\mathcal{X}_{Q,x} = \uplus_{u \in Q} \mathcal{X}_{u,x} (\triangleq [\dots, \mathcal{X}_{u,x}, \dots]) \in \mathbb{R}^{(m+1) \times |Q|}$. Note that there will be some $u \in Q$ such that $x \notin \mathcal{V}_u$, for which $\mathcal{X}_{u,x}$ is set to an all-zero vector. Through this procedure, the joined regular subgraph with query-level RPEs is fed into GPUs for model inference. More algorithmic intuition behind this can be found in Supp. B.

The data structure described in Sec.3.3 enables a highly parallel implementation of subgraph joining along with optimized memory management. On the CPU side, $\mathcal{X}_{Q,x}$ is not directly used to assemble the walks. Instead, we use a query-level RPE-ID that joins node-level RPE indices in \mathcal{T} , i.e. use $\text{RPE-ID}_{Q,x} = [\dots, \text{RPE-ID}_{u,x}, \dots] \in \mathbb{R}^{|Q|}$ for $u \in Q$, which reduces the memory cost from $(m+1) \times |Q|$ to $|Q|$. For instance, in Fig. 3 (bottom right), $\mathcal{X}_{Q,b} = ([0, 2, 0], [0, 2, 0])$ can be substituted by $\text{RPE-ID} = (2, 2)$, as the RPE-ID of $[0, 2, 0]$ in \mathcal{T} is 2, etc. To achieve this, SUREL pre-allocates an array with the fixed-size $[M \times m \times |Q|, |Q|]$, where $M \times m \times |Q|$ is the number of nodes in all the walks. Then, SUREL fills each entry of the array with $\text{RPE-ID}_{u,x}$ by multi-threads. Note that $\text{RPE-ID}_{u,x}$ can be retrieved via the dictionary operation $\mathcal{H}_u(x)$ rapidly. Collecting RPEs via RPE-IDs is later performed on GPUs in parallel via the indexing operation $\mathcal{X}_{u,x} = \mathcal{T}(\text{RPE-ID}_{u,x})$, where \mathcal{T} is pinned in GRAM earlier. As for implementation, SUREL incorporates a Python/C hybrid API built on top of NumPy, PyTorch, OpenMP and uthash.

Some remarks can be made here. First, the above algorithm contains some redundancy to compute the query-level RPE-ID for the nodes that appear multiple times in the walks. However, in practice, we find that around half nodes only appear once so such redundancy at most doubles the computing time. To avoid such redundancy, one may first compute the set union $\mathcal{V}_Q = \cup_{u \in Q} \mathcal{V}_u$ and then compute the query-level RPE-ID by traversing all the nodes in \mathcal{V}_Q . However, such a set union operation can be hardly to implement in parallel efficiently. When multithreading is enabled, we observe a significant increase in the efficiency of SUREL, as opposed to the set union operation. Furthermore, by dynamically adjusting the number of threads, the workload between CPU and GPU can be well balanced. Second, we empirically find that assembling walks using RPE-IDs instead of RPEs provides observable performance boost (speed up by $\times 2$ or more), otherwise data communication between CPU and GPU would be one of the bottlenecks.

3.5 Neural Encoding

After the subgraph joining for each query, the obtained subgraph is represented by a concatenated set of walks on which the nodes are paired with query-level RPEs (see Fig. 3). Next, we introduce neural networks to encode these walks into subgraph representation h_Q .

Due to its intrinsic regularity, any sequential models, e.g., MLP, CNN, RNN, and transformers can be adopted for sampled walks. We test RNN and MLP for neural encoding, both of which achieve similar results. Next, we take the RNN as an example. We encode each

walk $W = (w_0, w_1, \dots, w_m) \in \mathcal{W}$, where w_i 's denote the node at step i in one sampled walk as $\text{enc}(W) = \text{RNN}(\{f(X_{Q, w_i})\}_{i=0,1,\dots,m})$. Here, f is to encode the query-level RPE. To support node or edge attributes for each step $w_k \in W$, the above formulation can be extended by concatenating those attributes after its RPE. To obtain the final subgraph representation of Q , we aggregate the encoding of each associated set of walks through a mean pooling, i.e., $h_Q = \text{mean}(\{\text{enc}(W) | W \text{ starts from some } u \in Q\})$. In the end, a two-layer classifier is used to make the prediction by taking h_Q as the input. In our experiments, all the tasks can be formulated as binary classification, and thus we adopt Binary Cross Entropy (BCE) as the loss function.

3.6 The Training and Serving Pipelines

SUREL organically incorporates the storage designed in Sec. 3.3 and the subgraph-joining operation described in Sec. 3.4 to achieve efficient training and model serving.

Subgraph queries Q are sets of nodes, which often comes from a common ambient on a large graph. There might be many overlaps between different queries and their m -hop induced subgraphs. If the queried subgraphs are known in prior, we may put these queries with high node overlap into the same batch to improve data reuse. In practice, the test queries are usually given online while the training ones can be prepared in advance. Hence, we propose to accelerate the training pipeline by mini-batching the overlapping queries. Based on the specific situation, practitioners can choose a suitable pipeline accordingly. Algorithm 2 summarizes the overall training procedure of SUREL.

Mini-batching for Training. We first randomly sample a seed-set of nodes \mathcal{V} from the union of queried node sets $\cup Q$. Then, we run BFS to expand the seed-set \mathcal{V} . Neighbor fetching of the BFS here is based on the grouped queries instead of the original graph: a neighbor of node u is defined as the node that shares at least one query with u . During BFS, the reached queries will be added to the mini-batch \mathcal{B} . The expansion stops once the size of the seed-set \mathcal{V} or the size of the mini-batch \mathcal{B} reaches some pre-defined limits. Since the data structure for each query in SUREL after subgraph joining is regular, it is easy to decide the size limits of seed-set and mini-batch based on resource availability (i.e. GRAM). In practice, this BFS procedure improves reusability of data within each mini-batch, and may significantly decrease the communication cost between CPU and GPU.

Efficient Negative Query Sampling In many SGRL tasks, the training set only contains positive queries. For example, in link/motif prediction, the observed links/motifs are used as positive queries. Since negative training queries are not specified, randomly sampled missing links/motifs are generally used as negative queries. In our training pipeline, negative queries are randomly selected within the seed-set \mathcal{V} . With high probability, the randomly paired negative samples do not correspond to positive queries, and thus are safe to be used. This strategy enforces that negative queries always share nodes with positive ones, further improving data reuse.

4 EVALUATION

In this section, we aim to evaluate the following points:

Algorithm 2: The Training Pipeline of SUREL

Input: A graph \mathcal{G} , a set of training queries $\{(Q_i, y_i)\}$, batch capacity B_1 , batch size B_2
Output: A Neural Network for Neural Encoding $\text{NN}(\cdot)$

- 1 Prepare the collection of set of walks \mathcal{W} and RPEs \mathcal{X}
- 2 **for** $iter = 1, \dots, \text{max_iter}$ **do**
- 3 Initialize the set $Q = \emptyset$ to track reached queries;
- 4 Randomly choose a seed-set of nodes \mathcal{V} from $\cup Q$;
- 5 Run BFS to expand \mathcal{V} and Q until $|\mathcal{V}| = B_1$ or $|Q| = B_2$;
- 6 Generate negative training queries (if not given) for a mini-batch \mathcal{B} and put them into Q ;
- 7 Perform subgraph (RPE) joining for queries in Q ;
- 8 Encoding the concatenated walks by $\text{NN}(\cdot)$ to get the subgraph representation h_Q for each query;
- 9 Use BP algorithm to optimize model parameters.
- 10 **end**

- Regarding prediction performance, can SUREL outperform state-of-the-art SGRL models? Can SUREL significantly outperform canonical GNNs and transductive graph embedding methods due to the claimed benefit of SGRL?
- Regarding runtime, can SUREL significantly outperform state-of-the-art SGRL models? Can SUREL achieve comparable runtime performance compared to canonical GNNs? Previous SGRL models are typically much slower than canonical GNNs.
- How about the parameter sensitivity of SUREL? How do the hyper-parameters the walk length m and the number of walks M impact the overall performance?
- How does the parallel design of SUREL perform and scale?

4.1 Evaluation Setup

We conduct extensive experiments to evaluate the proposed framework with three kinds of graphs (homogeneous, heterogeneous, and higher-order homogeneous) on three corresponding types of tasks, namely, link prediction, relation prediction and higher-order pattern prediction. Homogeneous graphs are the graphs without node/link types. Heterogeneous graphs include node/link types. Higher-order graphs contain higher-order links that may connect more than 2 nodes. The dataset statistics are summarized in Table 2, most of which are larger than the datasets used in [57, 58], not to mention that our node-set prediction task is much more complex than the node classification task considered in previous works.

Open Graph Benchmark (OGB). We use three link prediction and one relation prediction datasets [16]: ppa - a protein interaction network, collab - a collaboration network, and citation2 - a citation network; and one heterogeneous network ogb-mag, which contains four types of nodes (paper, author, institution and field) and their relations extracted from MAG [42].

Higher-order Graph Dataset. DBLP-coauthor is a temporal higher-order network that records co-authorship of papers as time-stamped higher-order links. tags-math contains sets of tags that are applied to questions on the website math.stackexchange.com as higher-order links. For both higher-order graphs, SUREL and

Table 2: Summary Statistics and Experimental Setup for Evaluation Datasets.

Dataset	Type	#Nodes	#Edges	Avg. Node Deg.	Density	Split Ratio	Split Type	Metric
citation2	Homo.	2,927,963	30,561,187	20.7	0.00036%	98/1/1	Time	MRR
collab	Homo.	235,868	1,285,465	8.2	0.0046%	92/4/4	Time	Hits@50
ppa	Homo.	576,289	30,326,273	73.7	0.018%	70/20/10	Throughput	Hits@100
BALBc1	Homo./Bio	3,538,495	5,345,897	3.02	0.000085%	80/10/10	Random	ROC AUC
mag	Hetero.	Paper(P): 736,389 Author(A): 1,134,649	P-A: 7,145,660 P-P: 5,416,271	21.7	N/A	99/0.5/0.5	Time	MRR
tag-math	Higher.	1,629	91,685 (projected) 822,059 (hyperedges)	N/A	N/A	60/20/20	Time	MRR
DBLP-coauthor	Higher.	1,924,991	7,904,336 (projected) 3,700,067 (hyperedges)	N/A	N/A	60/20/20	Time	MRR

all the baselines will treat them as standard graphs by projecting higher-order links into cliques. However, the training and testing queries are generated based on higher-order links detailed next.

The dataset BALBc1 for brain vessel prediction is introduced in Sec. 4.6 as the experimental setting up is relatively independent and different.

Settings. For *Link Prediction*, we follow the data split policy as OGB requires to isolate the validation and testing links (queries) from the graphs. For *Relation Prediction*, the relations of paper-author (P-A) and paper-citation (P-P) are selected. The dataset is split based on timestamps. 0.5% of existing edges of each target relation type are selected from ogb-mag. For each paper, two authors/citations are picked from its P-A/P-P relations respectively, one for validation and the other for testing. The remaining links are used for training. For *Higher-order Pattern Prediction*, we focus on predicting whether two nodes will be connected to a third node concurrently via a higher-order link in the future. Specifically, positive queries are set as the node triplets, where two nodes are linked before the timestamp t and a third node establishes connection to the pair via a higher-order link after t . The split ratio of positive node triplets is 60/20/20 for training/validation/testing. For *Relation Prediction* and *Higher-order Pattern Prediction*, each positive query is paired with 1000 randomly sampled negative queries (except for tags-math that uses 100) in testing. For fair comparison, all baselines are tested on the fixed negative queries sampled individually for each task. All experiments are run 10 times independently, and we report the mean performance and standard deviations.

Baselines. We consider three classes of baselines. *Graph Embedding methods* for transductive learning: Node2vec [13], DeepWalk [32] and Marius [28, 46], which learns a single embedding for each node and may suffer from the information over-squashing issue; *Canonical GNNs*: GCN [20], GraphSAGE [15], GraphSAINT [52], Cluster-GCN [8], Relational GCN (R-GCN) [33], Relation-aware Heterogeneous Graph Neural Network (R-HGNN) [50]; *SGRL models*: SEAL[54], DE-GNN[22]. SEAL supports both offline and online subgraph extraction per query. However, offline subgraph extraction takes extensive time and massive memory (extracting 2% training samples alone of citation2 needs 2+ hours and 102GB RAM). Thus, we only keep the online setting for SEAL. DE-GNN only supports offline subgraph extraction per query. The detailed configuration of the baselines and SUREL (the network architectures

Table 3: Results for Link Prediction on OGB.

Models	citation2 MRR (%)	collab Hits@50 (%)	ppa Hits@100 (%)
Node2vec	61.28±0.15	47.54±0.78	18.05±0.52
DeepWalk	84.47±0.04	49.08±0.93	27.80±1.71
Marius	72.53±0.14	19.31±1.01	31.24±2.28
GCN	84.74±0.21	44.75±1.07	18.67±1.32
SAGE	82.60±0.36	54.63±1.12	16.55±2.40
Cluster-GCN	80.04±0.25	44.02±1.37	3.56±0.40
GraphSAINT	79.85±0.40	53.12±0.52	3.83±1.33
SEAL	<u>87.67±0.32</u>	63.64±0.71	<u>48.80±3.16</u>
SUREL	89.74±0.18	<u>63.34±0.52</u>	53.23±1.03

and hyper-parameters including the number of layers, hidden dimensions, learning rate, the number of sampled walks per node M and the walk length m) are summarized in Supp. C.3.

Metric. The evaluation metrics include Hits@K and Mean Reciprocal Rank (MRR). Hit@K counts the percentage of positive samples ranked at the top-K place against all the negative ones. MRR firstly calculates the inverse of the ranking of the first correct prediction against the given number of paired negative samples, and then an average is taken over the total queries.

Environment. We use a server with four Intel(R) Xeon(R) 24-Core Gold 6248R CPUs, 1TB DRAM, and eight NVIDIA QUADRO RTX 6000 (24GB) GPUs. Note that, when GCN and R-GCN adopt full-batch training, 24GB GPUs cannot load the entire graphs, so these two models use a NVIDIA Tesla A100 (48GB) GPU instead. SUREL may only achieve better performance if using the 48GB one.

4.2 Prediction Performance Analysis

Table 3 shows the link prediction results. Apparently, for these three benchmarks, the performance of SGRL models is significantly better than transductive graph embedding models and canonical GNNs, particularly for the challenging tasks in ppa and collab. Within SGRL models, SUREL sets two SOTA results on ppa and citation2, and get comparable performance on collab against SEAL, which validates the modeling effectiveness of our proposed walk-based framework.

Table 4: Results for Relation Prediction and Higher-order Pattern Prediction.

Models	MAG(P-A) MRR (%)	MAG(P-P) MRR (%)	tags-math MRR (%)	DBLP MRR (%)
GCN	39.43±0.29	57.43±0.30	51.64±0.27	37.95±2.59
SAGE	25.35±1.49	60.54±1.60	54.68±2.03	22.91±0.94
R-GCN	37.10±1.05	56.82±4.71	-	-
R-HGNN	33.41±2.47	45.91±3.28	-	-
DE-GNN	-	-	36.67±1.59	Timeout
SUREL	45.33±2.94	82.47±0.26	71.86±2.15	97.66±2.89

Table 5: Breakdown of the Runtime, Memory Consumption for Different Models on citation2, collab, and DBLP-coauthor. Training time is calculated if no better validation performance is observed in 3 consecutive epochs, which assumes the model has converged.

Models		Runtime (s)				Memory (GB)	
		Prep.	Train	Inf.	Total	RAM	GPU
citaitaion2	GCN	17	16,835	32	16,884	9.5	37.55
	Cluster-GCN	197	2,663	82	2,942	18.3	14.07
	GraphSAINT	140	3,845	86	4,071	16.9	14.77
	SEAL (1-hop)	46	22,296	130,312	152,654	36.5	3.35
	SUREL	31	2,096	7,959	10,086	15.2	4.50
collab	GCN	6	840	0.1	846	3.2	5.17
	Cluster-GCN	8	649	0.2	666	3.4	5.29
	GraphSAINT	<1	6,746	0.2	6,747	3.2	6.58
	SEAL (1-hop)	10	7,675	37	7,722	15.4	6.97
	SUREL	<1	1,720	8	1,728	3.6	5.57
DBLP	GCN	-	153	95	248	8.0	25.80
	SAGE	-	86	77	161	7.5	24.70
	SUREL	10	430	1,667	2,107	8.6	8.61

Table 4 shows the results for relation prediction and higher-order pattern prediction. We observe a large gap (up to 60%) between canonical GNNs and SUREL-based models, especially in high-order cases. This again demonstrates the inherent modeling limitation of canonical GNNs to predict over a set of nodes. DE-GNN adopts subgraph extraction to perform higher-order pattern prediction while suffering severe scalability issues. We try our best to deploy DE-GNN on these large graphs, while among the four graphs, it can only be applied to tags-math by using 10% training samples. DE-GNN takes more than 300 hours to even preprocess 5% training queries of DBLP-coauthor.

4.3 Runtime and Memory Complexity Analysis

Table 5 reports the running time, memory consumption comparison on a single machine (using one GPU) between canonical GNNs and SGRL models. SUREL offers a reasonable total running time on these benchmarks compared with canonical GNNs. Meanwhile, its preprocessing overhead is negligible, and the high-order case can be efficiently handled as well. SEAL adopts online extraction and thus

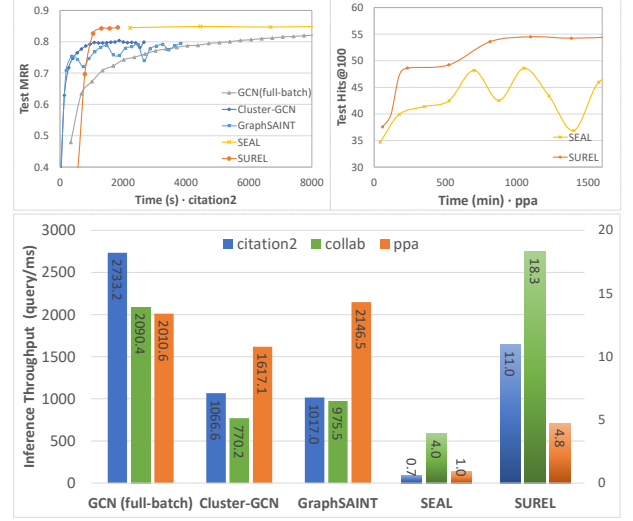


Figure 4: Performance Profiling of Training & Inference (Up: Time-to-accuracy; Down: Inference Throughput).

is efficient in preprocessing, while the training suffers from the computation bottleneck. DE-GNN uses offline extraction, and it takes 15+ hours and 98GB RAM to process training queries in tag-math, which is obviously incapable of scaling to DBLP-coauthor (so not present in Table 5). Overall, SUREL substantially accelerates the offline subgraph extraction and makes it feasible for SGRL on large graphs. In terms of memory management, SUREL achieves comparable RAM usage to canonical GNNs, because the number of walks M and the steps m are small constants in practice. The extra memory cost is linear in $|\mathcal{V}|$, so the total memory cost is still dominated by the original graph. However, SEAL induces much more RAM usage as it extracts subgraphs of long-tail sizes and the total memory cost is often sup-linear in $|\mathcal{V}|$. Both SEAL and SUREL consume much less GPU memory because they do not need GPU to load large adjacency matrices and host node representations.

We further profile the training and inference performance and present it in Fig. 4. The upper half plots the time-to-accuracy comparison between canonical GNNs and SGRL models. Each dot indicates one training epoch for full-batch GCN, SEAL and SUREL, 10 training epochs for Cluster-GCN and GraphSAINT. As it shows, both SEAL and SUREL use 1-3 epochs to get good enough performance, and each epoch of SUREL takes around 1/10 time of SEAL on citation2. However, the curve of SEAL is pretty fluctuating on ppa, which leads to longer convergence. SUREL uses large M and m to achieve better and more stable performance on ppa, so the per epoch training time is comparable with SEAL. The time per epoch of the full-batch GCN is comparable with SUREL, while Cluster-GCN and GraphSAINT are faster. However, these models generally take longer time to converge to even subpar performance. We do not plot the training curves of canonical GNN baselines for ppa because of their poor performance (see Table 3).

The bottom half of Fig. 4 provides the comparison of end-to-end inference throughput between two classes of models. Canonical

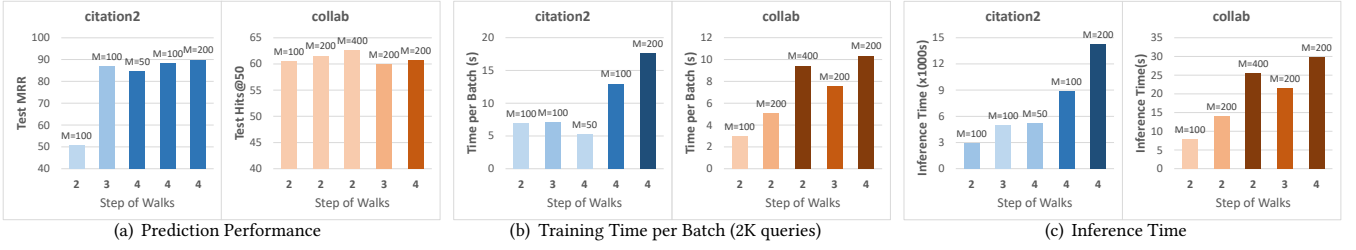


Figure 5: Hyper-parameter Analysis: the number of walks M ; the step of walks m .

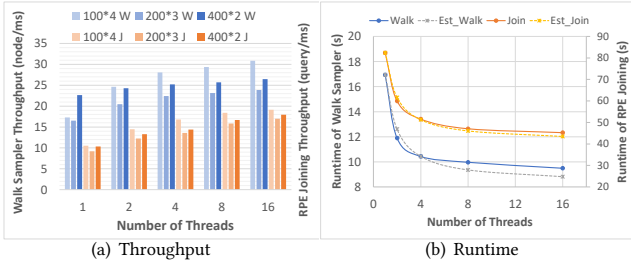


Figure 6: Performance Scaling of SUREL (Walk Sampler and Query-level RPE Joining) against Number of Threads.

GNNs offer rapid inference, since they generate node representations as the intermediate computation results that are shared across all queries. But as aforementioned, sharing node representations may over-squash useful information and degenerate performance as shown in Table 3. SEAL, as SGRL, achieves good prediction performance but its inference is extremely slow, because a subgraph extraction operation has to be done for each query. SUREL fundamentally renovates it by replacing the subgraph extraction with walk-based joining. It brings up to 4 – 16 \times speedup on inference compared with SEAL for link prediction, and even more speedup than DE-GNN for higher-order pattern prediction.

4.4 Significant Hyperparameter Analysis

The number M and the step m of walks effect the scalability and accuracy of SUREL. To examine their impact, we evaluate SUREL on citation2, a large sparse graph, and collab, a medium dense graph, for different values of M and m .

Prediction Performance. Fig. 5(a) shows the prediction results. As we expected, the performance consistently increases if we use larger number of walks M . But for the step m , it is not necessary that longer steps will guarantee better results, which depends on the specifics of the dataset. For instance, in network citation2, to accurately predict the link between two papers, more steps are needed as it would capture a larger group of papers which share similar semantics. While for collab, the case is different, as deeper walks would include more noise for predicting collaborations between two authors. In general, some small m (2 ~ 5) and M (50 ~ 400) ensure good enough performance. By adjusting m and M , we can achieve the trade-off between accuracy, complexity, and scalability, which is not an option for other SGRL models.

Training and Inference Time Cost. As Figs. 5(b) and 5(c) demonstrated, the time of walk sampling and subgraph joining is nearly linear w.r.t. the total number of walks ($m * M$) under the same number of threads (16 by default). Here, we do not regulate M based on the degree of each node in the query, which may induce certain duplication in sampled walks originated from the nodes with small degrees. Using degree-adaptive M is promising to improve the scalability of SUREL while keeping good prediction performance. We leave such investigation for future study.

4.5 Performance Scaling

To investigate the scaling performance of the parallel implementation, we examine the runtime of bottleneck operations in SUREL by using different number of threads. Fig. 6(a) shows the throughput of walk sampler and query-level RPE joining on citation2. The runtime is also compared to the estimated runtime by Amdahl’s law [12] shown in Fig. 6(b): walk sampling and RPE joining achieve good agreement with the expected speedup, and thus imply well parallelized implementation.

4.6 Case Study: Brain Vessel Prediction

The whole brain vessel graph [31] is extracted and constructed from the mouse brain, illustrating the spatial organization of the brain’s microvasculature. The structure of vessels plays a vital role in neuroscience, which can be used for detecting various diseases (e.g. Alzheimer’s and stroke) in the early stage. This ultra-large, spatial, structured biological graph benchmark is ideal to examine generalization and scalability of SGRL approaches in scientific discovery tasks. Following the experimental settings introduced by Paetzold et al. [31] (detailed in Supp. C.1), Table 6 shows the results of SEAL and SUREL for vessel (link) prediction on the dataset BALBc1 [39]. Both SGRL approaches reach high accuracy with strong inductive bias, which significantly outperform traditional methods and canonical GNNs reported in [31]. Compared with SEAL, SUREL achieves over 56 \times speedup in training and over 6 \times in testing, which further validates its superior efficiency for subgraph learning and versatile applicability on various types of large-scale graph learning tasks.

5 CONCLUSION

We propose a novel computational paradigm, SUREL for subgraph-based representation learning over large-scale graphs. SUREL targets predicting relations over the node sets. It decouples graph

Table 6: Results for Vessel Prediction on BALBc-1.

Models	Runtime (s)		ROC AUC (%)	
	Train	Inf.	Valid	Test
SEAL	8,724	1,096	91.05±0.01	91.00±0.01
SUREL	154	175	91.42±0.02	91.34±0.01

structures into sets of walks to avoid the long-tail issue of sub-graph sizes and improve data reuse. Then, it uses relative positional encoding to re-join the decomposed subgraph for each queried node set. Both steps allow for full parallelization and significantly improve the model scalability. SUREL incorporates the principle of algorithm-system codesign, which releases the full potential of limited resources for learning on large-scale data. To the best of our knowledge, this is the first work from the perspective of system scalability to investigate subgraph-based representation learning. Experiments also show that SUREL achieves superior performance in both prediction and scalability for three different SGRL tasks over seven large, real-world graph benchmarks.

REFERENCES

- [1] Uri Alon and Eran Yahav. 2020. On the bottleneck of graph neural networks and its practical implications. In *International Conference on Learning Representations*.
- [2] Michael L Bates, Susan M Bengtson Nash, Darryl W Hawker, John Norbury, Jonny S Stark, and Roger A Cropp. 2015. Construction of a trophically complex near-shore Antarctic food web model using the Conservative Normal framework with structural coexistence. *Journal of Marine Systems* 145 (2015), 1–14.
- [3] Rachel E Bennett, Ashley B Robbins, Miwei Hu, Xinrui Cao, Rebecca A Betensky, Tim Clark, Sudeshna Das, and Bradley T Hyman. 2018. Tau induces blood vessel abnormalities and angiogenesis-related gene expression in P301L transgenic mice and human Alzheimer’s disease. *Proceedings of the National Academy of Sciences* 115, 6 (2018), E1289–E1298.
- [4] Giorgos Bouritsas, Fabrizio Frasca, Stefanos Zafeiriou, and Michael M Bronstein. 2020. Improving graph neural network expressivity via subgraph isomorphism counting. In *ICML 2020 Workshop on Graph Representation Learning and Beyond*.
- [5] Jie Chen, Tengfei Ma, and Cao Xiao. 2018. Fastgcn: fast learning with graph convolutional networks via importance sampling. In *International Conference on Learning Representations*.
- [6] Jianfei Chen, Jun Zhu, and Le Song. 2018. Stochastic training of graph convolutional networks with variance reduction. In *International Conference on Machine Learning*. PMLR, 942–950.
- [7] Zhengdao Chen, Lei Chen, Villar Soledad, and Joan Bruna. 2020. Can Graph Neural Networks Count Substructures?. In *Advances in Neural Information Processing Systems*, Vol. 33.
- [8] Wei-Lin Chiang, Xuanqing Liu, Si Si, Yang Li, Samy Bengio, and Cho-Jui Hsieh. 2019. Cluster-gcn: An efficient algorithm for training deep and large graph convolutional networks. In *Proceedings of the 25th ACM SIGKDD International Conference on Knowledge Discovery & Data Mining*. 257–266.
- [9] Alessandro Epasto and Bryan Perozzi. 2019. Is a single embedding enough? learning node representations that capture multiple social contexts. In *The world wide web conference*. 394–404.
- [10] Eszter Farkas, Gineke I De Jong, Rob AI de Vos, Ernst NH Jansen Steur, and Paul GM Luiten. 2000. Pathological features of cerebral cortical capillaries are doubled in Alzheimer’s disease and Parkinson’s disease. *Acta neuropathologica* 100, 4 (2000), 395–402.
- [11] Matthias Fey and Jan Eric Lenssen. 2019. Fast Graph Representation Learning with PyTorch Geometric. In *ICLR 2019 Workshop on Representation Learning on Graphs and Manifolds*.
- [12] Ananth Grama, Vipin Kumar, Anshul Gupta, and George Karypis. 2003. *Introduction to parallel computing*. Pearson Education.
- [13] Aditya Grover and Jure Leskovec. 2016. node2vec: Scalable feature learning for networks. In *Proceedings of the 22nd ACM SIGKDD International Conference on Knowledge Discovery & Data Mining*. 855–864.
- [14] William L Hamilton. 2020. Graph representation learning. *Synthesis Lectures on Artificial Intelligence and Machine Learning* 14, 3 (2020), 1–159.
- [15] William L Hamilton, Rex Ying, and Jure Leskovec. 2017. Inductive representation learning on large graphs. In *Proceedings of the 31st International Conference on Neural Information Processing Systems*. 1025–1035.
- [16] Weihua Hu, Matthias Fey, Marinka Zitnik, Yuxiao Dong, Hongyu Ren, Bowen Liu, Michele Catasta, and Jure Leskovec. 2020. Open Graph Benchmark: Datasets for Machine Learning on Graphs. *arXiv preprint arXiv:2005.00687* (2020).
- [17] Kexin Huang and Marinka Zitnik. 2020. Graph meta learning via local subgraphs. In *Advances in Neural Information Processing Systems*, Vol. 33.
- [18] Wenbing Huang, Tong Zhang, Yu Rong, and Junzhou Huang. 2018. Adaptive Sampling Towards Fast Graph Representation Learning. In *Advances in Neural Information Processing Systems*, Vol. 31.
- [19] Zhihao Jia, Sina Lin, Mingyu Gao, Matei Zaharia, and Alex Aiken. 2020. Improving the accuracy, scalability, and performance of graph neural networks with roc. *Proceedings of Machine Learning and Systems* 2 (2020), 187–198.
- [20] Thomas N Kipf and Max Welling. 2017. Semi-supervised classification with graph convolutional networks. In *International Conference on Learning Representations*.
- [21] Daphne Koller, Nir Friedman, Sašo Džeroski, Charles Sutton, Andrew McCallum, Avi Pfeffer, Pieter Abbeel, Ming-Fai Wong, Chris Meek, Jennifer Neville, et al. 2007. *Introduction to statistical relational learning*. MIT press.
- [22] Pan Li, Yanbang Wang, Hongwei Wang, and Jure Leskovec. 2020. Distance Encoding: Design Provably More Powerful Neural Networks for Graph Representation Learning. In *Advances in Neural Information Processing Systems*, Vol. 33.
- [23] David Liben-Nowell and Jon Kleinberg. 2007. The link-prediction problem for social networks. *Journal of the American society for information science and technology* 58, 7 (2007), 1019–1031.
- [24] Husong Liu, Shengliang Lu, Xinyu Chen, and Bingsheng He. 2020. G3: when graph neural networks meet parallel graph processing systems on GPUs. *Proceedings of the VLDB Endowment* 13, 12 (2020), 2813–2816.
- [25] Xin Liu, Haojie Pan, Mutian He, Yangqiu Song, Xin Jiang, and Lifeng Shang. 2020. Neural subgraph isomorphism counting. In *Proceedings of the 26th ACM SIGKDD International Conference on Knowledge Discovery & Data Mining*. 1959–1969.
- [26] Yunyu Liu, Jianzhu Ma, and Pan Li. 2022. Neural Higher-order Pattern (Motif) Prediction in Temporal Networks. In *Proceedings of the Web Conference 2022*.
- [27] Zhaoyu Lou, Jiaxuan You, Chengtao Wen, Arquimedes Canedo, Jure Leskovec, et al. 2020. Neural Subgraph Matching. *arXiv preprint arXiv:2007.03092* (2020).
- [28] Jason Mohoney, Roger Waleffe, Henry Xu, Theodoros Rekatsinas, and Shivaram Venkataraman. 2021. Marius: Learning Massive Graph Embeddings on a Single Machine. In *15th USENIX Symposium on Operating Systems Design and Implementation (OSDI 21)*. 533–549.
- [29] Christopher Morris, Martin Ritzert, Matthias Fey, William L Hamilton, Jan Eric Lenssen, Gaurav Rattan, and Martin Grohe. 2019. Weisfeiler and leman go neural: Higher-order graph neural networks. In *Proceedings of the AAAI Conference on Artificial Intelligence*, Vol. 33. 4602–4609.
- [30] Kenta Oono and Taiji Suzuki. 2019. Graph Neural Networks Exponentially Lose Expressive Power for Node Classification. In *International Conference on Learning Representations*.
- [31] Johannes C Paetzold, Julian McGinnis, Suprosanna Shit, Ivan Ezhov, Paul Büschl, Chinmay Prabhakar, Anjany Sekuboyina, Mihail Todorov, Georgios Kaissis, Ali Ertürk, et al. 2021. Whole Brain Vessel Graphs: A Dataset and Benchmark for Graph Learning and Neuroscience. In *Thirty-fifth Conference on Neural Information Processing Systems Datasets and Benchmarks Track (Round 2)*.
- [32] Bryan Perozzi, Rami Al-Rfou, and Steven Skiena. 2014. Deepwalk: Online learning of social representations. In *Proceedings of the 20th ACM SIGKDD International Conference on Knowledge Discovery & Data Mining*. 701–710.
- [33] Michael Schlichtkrull, Thomas N Kipf, Peter Bloem, Rianne Van Den Berg, Ivan Titov, and Max Welling. 2018. Modeling relational data with graph convolutional networks. In *European semantic web conference*. Springer, 593–607.
- [34] Balasubramaniam Srinivasan and Bruno Ribeiro. 2020. On the Equivalence between Node Embeddings and Structural Graph Representations. In *International Conference on Learning Representations*.
- [35] Nils Chr Stenseth, Wilhelm Falck, Ottar N Bjørnstad, and Charles J Krebs. 1997. Population regulation in snowshoe hare and Canadian lynx: asymmetric food web configurations between hare and lynx. *Proceedings of the National Academy of Sciences* 94, 10 (1997), 5147–5152.
- [36] Susan M Sunkin, Lydia Ng, Chris Lau, Tim Dolbeare, Terri L Gilbert, Carol L Thompson, Michael Hawrylycz, and Chinh Dang. 2012. Allen Brain Atlas: an integrated spatio-temporal portal for exploring the central nervous system. *Nucleic Acids Research* 41, D1 (2012), D996–D1008.
- [37] Komal Teru, Etienne Denis, and Will Hamilton. 2020. Inductive relation prediction by subgraph reasoning. In *International Conference on Machine Learning*. PMLR, 9448–9457.
- [38] John Thorpe, Yifan Qiao, Jonathan Eyolfson, Shen Teng, Guanzhou Hu, Zhihao Jia, Jinliang Wei, Keval Vora, Ravi Netravali, Miryung Kim, and Guoqing Harry Xu. 2021. Dorylus: Affordable, Scalable, and Accurate GNN Training with Distributed CPU Servers and Serverless Threads. In *15th USENIX Symposium on Operating Systems Design and Implementation (OSDI 21)*. 495–514.
- [39] Mihail Ivlilov Todorov, Johannes Christian Paetzold, Oliver Schoppe, Giles Tetteh, Suprosanna Shit, Velizar Efremov, Katalin Todorov-Völgyi, Marco Düring, Martin Dichgans, Marie Piraud, et al. 2020. Machine Learning Analysis of Whole Mouse Brain Vasculature. *Nature Methods* 17, 4 (2020), 442–449.

- [40] Marjolaine Uginet, Gautier Breville, Jérémy Hofmeister, Paolo Machi, Patrice H Lalive, Andrea Rosi, Aikaterini Fitsiori, Maria Isabel Vargas, Frederic Assal, Gilles Allali, et al. 2021. Cerebrovascular complications and vessel wall imaging in COVID-19 encephalopathy—a pilot study. *Clinical neuroradiology* (2021), 1–7.
- [41] Petar Veličković, Guillem Cucurull, Arantxa Casanova, Adriana Romero, Pietro Lio, and Yoshua Bengio. 2018. Graph attention networks. In *International Conference on Learning Representations*.
- [42] Kuansan Wang, Zhihong Shen, Chiyuan Huang, Chieh-Han Wu, Yuxiao Dong, and Anshul Kanakia. 2020. Microsoft academic graph: When experts are not enough. *Quantitative Science Studies* 1, 1 (2020), 396–413.
- [43] Minjie Wang, Lingfan Yu, Da Zheng, Quan Gan, Yu Gai, Zihao Ye, Mufei Li, Jinjing Zhou, Qi Huang, Chao Ma, et al. 2019. Deep Graph Library: Towards Efficient and Scalable Deep Learning on Graphs. (2019).
- [44] Xiyuan Wang and Muhan Zhang. 2022. GLASS: GNN with Labeling Tricks for Subgraph Representation Learning. In *International Conference on Learning Representations*.
- [45] Yanbang Wang, Yen-Yu Chang, Yunyu Liu, Jure Leskovec, and Pan Li. 2021. Inductive Representation Learning in Temporal Networks via Causal Anonymous Walks. In *International Conference on Learning Representations*.
- [46] Anze Xie, Anders Carlsson, Jason Mohoney, Roger Waleffe, Shanan Peters, Theodoros Rekatsinas, and Shivaram Venkataraman. 2021. Demo of marius: a system for large-scale graph embeddings. *Proceedings of the VLDB Endowment* 14, 12 (2021), 2759–2762.
- [47] Keyulu Xu, Weihua Hu, Jure Leskovec, and Stefanie Jegelka. 2019. How Powerful are Graph Neural Networks?. In *International Conference on Learning Representations*.
- [48] Hongxia Yang. 2019. Aligraph: A comprehensive graph neural network platform. In *Proceedings of the 25th ACM SIGKDD International Conference on Knowledge Discovery & Data Mining*. 3165–3166.
- [49] Rex Ying, Ruining He, Kaifeng Chen, Pong Eksombatchai, William L Hamilton, and Jure Leskovec. 2018. Graph convolutional neural networks for web-scale recommender systems. In *Proceedings of the 24th ACM SIGKDD International Conference on Knowledge Discovery & Data Mining*. 974–983.
- [50] Le Yu, Leilei Sun, Bowen Du, Chuanren Liu, Weifeng Lv, and Hui Xiong. 2021. Heterogeneous Graph Representation Learning with Relation Awareness. *arXiv preprint arXiv:2105.11122* (2021).
- [51] Hanqing Zeng, Muhan Zhang, Yinglong Xia, Ajitesh Srivastava, Andrey Malevich, Rajgopal Kannan, Viktor Prasanna, Long Jin, and Ren Chen. 2021. Decoupling the Depth and Scope of Graph Neural Networks. *Advances in Neural Information Processing Systems* 34 (2021).
- [52] Hanqing Zeng, Hongkuan Zhou, Ajitesh Srivastava, Rajgopal Kannan, and Viktor Prasanna. 2020. Graphsaint: Graph sampling based inductive learning method. In *International Conference on Learning Representations*.
- [53] Dalong Zhang, Xin Huang, Ziqi Liu, Jun Zhou, Zhiyang Hu, Xianzheng Song, Zhibang Ge, Lin Wang, Zhiqiang Zhang, and Yuan Qi. 2020. AGL: a scalable system for industrial-purpose graph machine learning. *Proceedings of the VLDB Endowment* 13, 12 (2020), 3125–3137.
- [54] Muhan Zhang and Yixin Chen. 2018. Link prediction based on graph neural networks. In *Advances in Neural Information Processing Systems*, Vol. 31.
- [55] Muhan Zhang and Yixin Chen. 2020. Inductive Matrix Completion Based on Graph Neural Networks. In *International Conference on Learning Representations*.
- [56] Muhan Zhang, Pan Li, Yinglong Xia, Kai Wang, and Long Jin. 2021. Labeling Trick: A Theory of Using Graph Neural Networks for Multi-Node Representation Learning. *Advances in Neural Information Processing Systems* 34 (2021).
- [57] Wentao Zhang, Zhi Yang, Yexin Wang, Yu Shen, Yang Li, Liang Wang, and Bin Cui. 2021. GRAIN: Improving Data Efficiency of Graph Neural Networks via Diversified Influence Maximization. *Proceedings of the VLDB Endowment* 14, 11 (2021), 2473–2482.
- [58] Hongkuan Zhou, Ajitesh Srivastava, Hanqing Zeng, Rajgopal Kannan, and Viktor Prasanna. 2021. Accelerating Large Scale Real-Time GNN Inference Using Channel Pruning. *Proceedings of the VLDB Endowment* 14, 9 (2021), 1597–1605.

A FURTHER ANALYSIS

Fig. 7 shows the degree distribution and the node size of subgraph with respect to different numbers of hops in real-world networks collab and citation2. The node size of subgraph dramatically increases when the hop $m \geq 2$, because many nodes have significantly large degrees in real-world networks as the left half of Fig. 7 illustrated. This leads to the size “explosion” issue for current SGRL models. Accordingly, most of SGRL models including SEAL [54, 56] and DE-GNN [22] can only accommodate up to 1-hop neighbors over large networks to avoid the scalability crisis, which in return

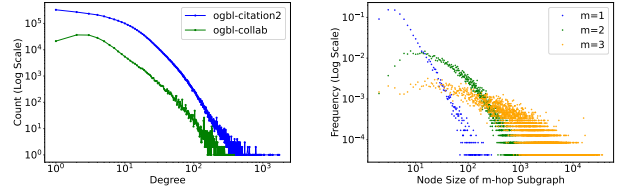


Figure 7: Characteristics of Real-World Networks

compromises their performance. SUREL solves this issue by breaking the subgraph into regular walks, which enables it to reach up to m -hop neighbors via m -step random walks. The long-hop neighbors give extra information, which is beneficial for improving the prediction performance.

B LIMITATIONS OF CANONICAL GNNs AND MORE ILLUSTRATION OF THE ALGORITHMIC INSIGHTS OF SUREL

Canonical GNNs are known to have several limitations, such as limited expressive power [29, 47], feature oversmoothing [30], information over-squashing[1] and noise contaminating with a large receptive field [17].

One of the biggest limitations is that canonical GNNs cannot distinguish the nodes that can be mapped to each other under some graph automorphism. For example, the nodes w and v in Fig. 1 satisfy this property, and canonical GNNs will associate them with the same node representations. Another more practical example from a real-world network is shown in Fig. 8. Although most large networks do not have non-trivial automorphism in practice, such nodes are not that common. However, the above issue of GNNs actually induces a more severe concern: the node representations learnt by GNNs cannot well capture the intra-node distance information which is crucial to predict over a set of nodes.

Another issue of canonical GNNs is to over-squash information into a single node representation. Node representations can be viewed as intermediate computation results that are often used in several downstream tasks. However, a node representation, if it carries the information that is suitable for one task, may carry subpar information for another task.

The third issue of canonical GNNs is the entanglement of the number of GNN layers and the range of the receptive field. In practice, when more complex and non-linear functions are to be approximated, one may want to add more layers to the neural network. However, GNNs adding more layers will also enlarge the receptive field that may introduce noise.

The last two issues of GNNs are demonstrated in the left column of Fig. 9. SGRL methods can handle the other two issues of GNNs in a simple way as illustrated in the right column of Fig. 9.

Moreover, to handle the challenge encountered in Fig. 1a, Fig. 1b indicates SGRL methods can be adopted. Note that the joint subgraph around the two target nodes ($\{u, w\}$ or $\{u, v\}$) should be considered as a whole. Subgraph extraction can be mathematically viewed as adding an intra-node distance feature to each node z : suppose $Q = \{u, w\}$ is the queried node set; if the distances from z

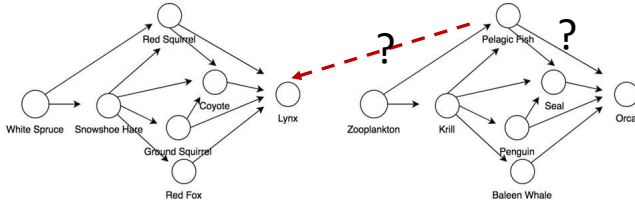


Figure 8: A food web example showing two disconnected components - the boreal forest [35] and the antarctic fauna [2]. The query here is which one is more likely the predator of Pelagic Fish, Lynx or Orca? Canonical GNNs cannot solve this query. Srinivasan and Ribeiro [34] explains this as the failure of GNNs to establish the correlation between the node representations.

to u and w are both less than or equal to 1, z will be selected. Such distance features can also be used as extra node features directly attached to the original node features. Li et al. [22] theoretically prove the effectiveness of using intra-node distance to better GNN expressive power. Our method SUREL is able to capture such intra-node distance by adopting relative positional encoding (RPEs). Lastly, we illustrate how SUREL is related to previous SGRL approaches in Fig. 10.

C ADDITIONAL EXPERIMENTAL SETTINGS

C.1 More Details about the Datasets

We choose OGB datasets² to evaluate our framework and other baselines, since it comes with large, real-world graphs (million of nodes/edges) with realistic applications (i.e. network of academic, proteins). Moreover, it provides standard, open-sourced evaluation metrics and tools for benchmarking.

Following the format of OGB, we construct four prediction tasks of relations and high-order patterns on heterogeneous graphs and hypergraphs³ respectively. The statistics and experimental setup of these tasks are summarized in Table 7. The original ogb-mag only contains features for ‘paper’-type nodes. We add the node embedding provided by [50] as the feature for the rest type of nodes in MAG(P-A)/(P-P). For the four tasks listed in Table 7, the model is evaluated by one positive query paired with certain number of randomly sampled negative queries. For fair comparison, all the baselines use the fixed negative queries that individually get sampled for each task above.

The whole brain vessel graph dataset [31] consists of 17 graphs from 2 different imaging modalities. Each node either represents an end point or the bifurcation of vessel branches. For each node, the physical location (real-valued coordinates of nodes in 3D space) and the anatomical location (one-hot encoded) in reference to the Allen brain atlas [36] are provided as node features. Each edge represents a vessel or a vessel segment which connects two nodes. The goal of vessel prediction is to determine the existence of a given vessel. In neuroscience, understanding the organization and changes of brain vessel is crucial to capture the early signs of various

Table 7: Dataset Statistics and Splitting for the Four Tasks on Relation Prediction and High-order Pattern Prediction.

Dataset	Query Type	#Train (Pos.)	#Val/Test (Pos.)	Pos./Neg. Ratio
MAG(P-A)	relation	6,519,308	16,180	1:1000
MAG(P-P)	relation	5,199,201	22,639	1:1000
tag-math	higher-order	74,955	24,985	1:100
DBLP-coauthor	higher-order	79,566	26,522	1:1000

pathologies, such as Alzheimer’s disease [3, 10] or even COVID-19 encephalopathy [40]. However, due to artifacts and shortcoming of the segmentation and network extraction of brain vasculature, the extracted graph may be over- or under-connected. Thus, this task is greatly useful in correcting missing and imperfect vessel graph connections. In our experiment on this brain vessel graph, we follow the setting in the benchmark paper [31]. Negative edges are non-existent but theoretically probable links between vessel branches. Further, Paetzold et al. [31] restricts the sampling of negative edges to a coordinate space which spatially surrounds the source node, and the target node is randomly selected within this cubic space around the source node. The ratio of positive and spatially sampled negative edges are balanced.

C.2 More Details about the Baselines

For link prediction and relation prediction, we select baselines from the current OGB leaderboard⁴ based on two major factors: scalability and performance. All the models from the leaderboard have released their code and the paper attached. We adopt the published number if available on the leaderboard with additional verification. For the rest, we use their official implementation with tuned parameters for model benchmarking as listed below.

- **Graph embedding:** graph embedding models for transductive learning such as Node2vec [13], DeepWalk⁵ [32]. As implicit matrix factorization, it can be extensively optimized, which enables it for large-scale graph mining tasks. The obtained node representation embeds the global positioning of target nodes in the given graph, which potentially can be exploited for link prediction. Marius⁶ [28] as one of SOTA frameworks that computes large-scale graph embeddings on a single machine with comparable accuracy but up to one order of magnitude faster than industrial systems.
- **GCN family:** a Graph Auto-Encoder model that using graph convolution layer to learning node representations, including GCN [20], GraphSAGE [15], and the derived models, such as Cluster-GCN [8], GraphSAINT [52].
- **R-GCN**⁷ [33]: a relational GCN that models relation graphs with node/link types.
- **R-HGNN**⁸ [50]: a heterogeneous GNN that focuses on learning relation-aware node representations with attention mechanism.
- **SEAL**⁹ [54]: apply GCN with double radius labeling tricks to obtain subgraph-level readout. SEAL reigns in the top spots of

⁴https://ogb.stanford.edu/docs/leader_linkprop/

⁵<https://github.com/dmlc/dgl/tree/master/examples/pytorch/ogb/deepwalk>

⁶<https://github.com/marius-team/marius>

⁷https://github.com/pyg-team/pytorch_geometric/blob/master/examples

⁸<https://github.com/yule-BUAA/R-HGNN/>

⁹https://github.com/facebookresearch/SEAL_OGB

²https://ogb.stanford.edu/docs/dataset_overview/

³<https://www.cs.cornell.edu/~arb/data/>

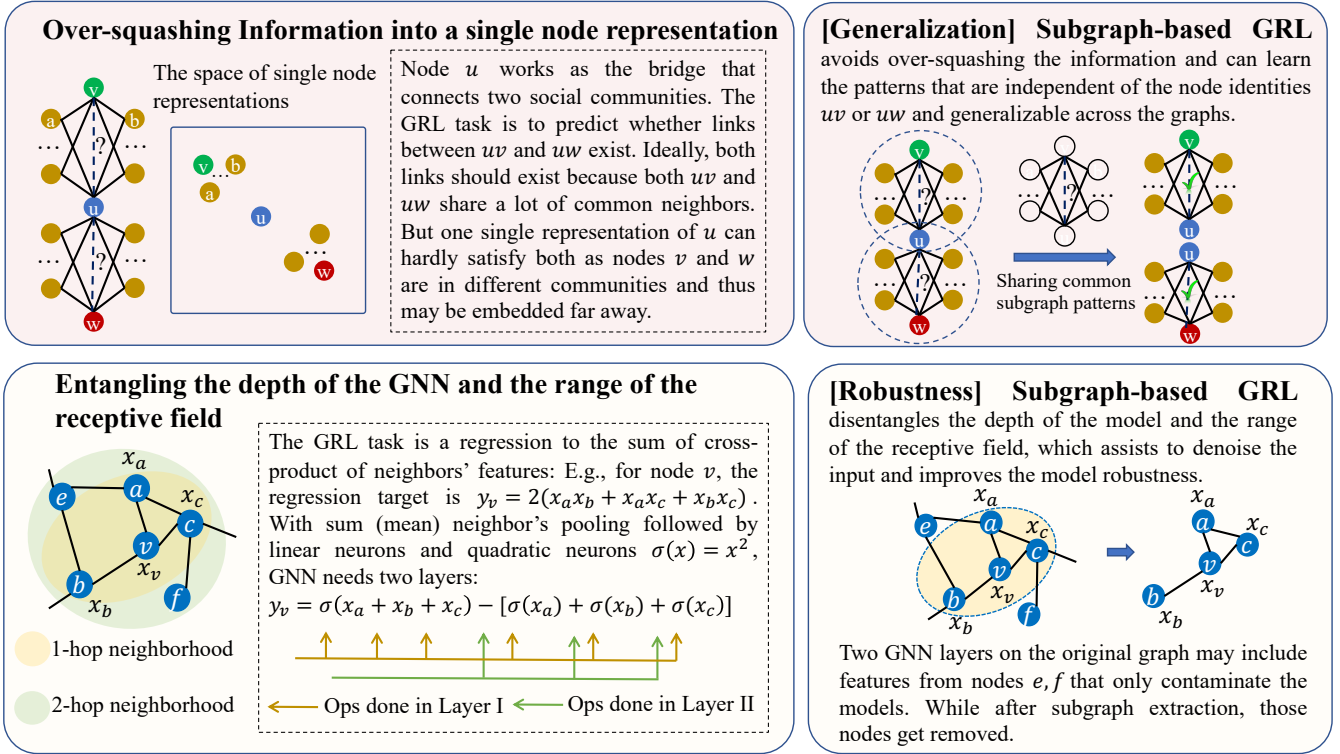


Figure 9: Two Limitations of Canonical-GNN-based GRL (Left) and How Do They Get Solved by Using Subgraph-based GRL (Right).

OGB leaderboard on multiple tasks, thanks to the expressiveness inherited from SGRL. The implementation we tested is specially optimized for OGB datasets provided in [56].

- **DE-GNN**¹⁰ [22]: a provably more powerful SGRL that utilizes distance features (shortest path distance, landing probability) to assist GNNs in representing any set of nodes. DE-GNN can be applied to tasks such as node classification, link prediction and high-order cases, with great performance.

For graph embedding approaches, we first use these models to generate node embeddings, and then train an MLP using DistMult as the decoder to obtain predictions. Then, as OGB standard protocol required, to perform data splitting, tune the MLP on the validation set, and evaluate them through the benchmark toolkit. All canonical GNN baselines¹¹ come with 3 message passing layers with 256 hidden dimensions, and a tuned dropout ratio in $\{0, 0.5\}$ for the full-batch training. Canonical GNN models use pairwise node embeddings as the representations of link/hyperedge, and then feed these representations into an MLP classifier for the final prediction. Besides, they need to use full training data to generate robust node representations. The hypergraph datasets do not come with node features. Thus, the canonical GNNs here use random features as the input for training along with other model parameters. R-GCN and R-GNN use relational GCNConv layers that support message

passing with different relation types between nodes. The relation type of edges is used as the input beside node features. SGRL-based models only use partial train set. Both SEAL and DE-GNN extract 1-hop enclosing subgraphs for training. SEAL applies 3 GCN layers with 32 hidden dimensions plus a sortpooling and several 1D convolution layers to generate the readout of subgraphs. DE-GNN adopts the shortest path distance calculated from each subgraph as the input feature, and then employs 2 TAGConv layers with 100 hidden dimensions to generate the readout of the target node set.

C.3 Architecture and Hyperparameter

SUREL consists of a 2-layer MLP with ReLU activation for the embedding of node RPEs and a 2-layer RNN to encode joint walks returned from queried subgraph joining. The hidden dimension of both networks is set to 64. Lastly, the concatenated encoding of the queried node set are fed into an 2-layer MLP classifier to make the final prediction.

For link prediction and relation prediction, we follow the inductive setting. Over the training graph, we randomly sample 5% links as positive training queries, each paired with k -many negative samples ($k = 50$ by default). We remove these links and use the remaining 95% links to sample walks and compute node RPE via Algorithm 1. For high-order pattern prediction, we use the given graph before timestamp t to generate RPE, and then optimize the model parameters by higher-order triplets provided in the train set.

¹⁰<https://github.com/snap-stanford/distance-encoding>

¹¹<https://github.com/snap-stanford/ogb/tree/master/examples/linkproppred>

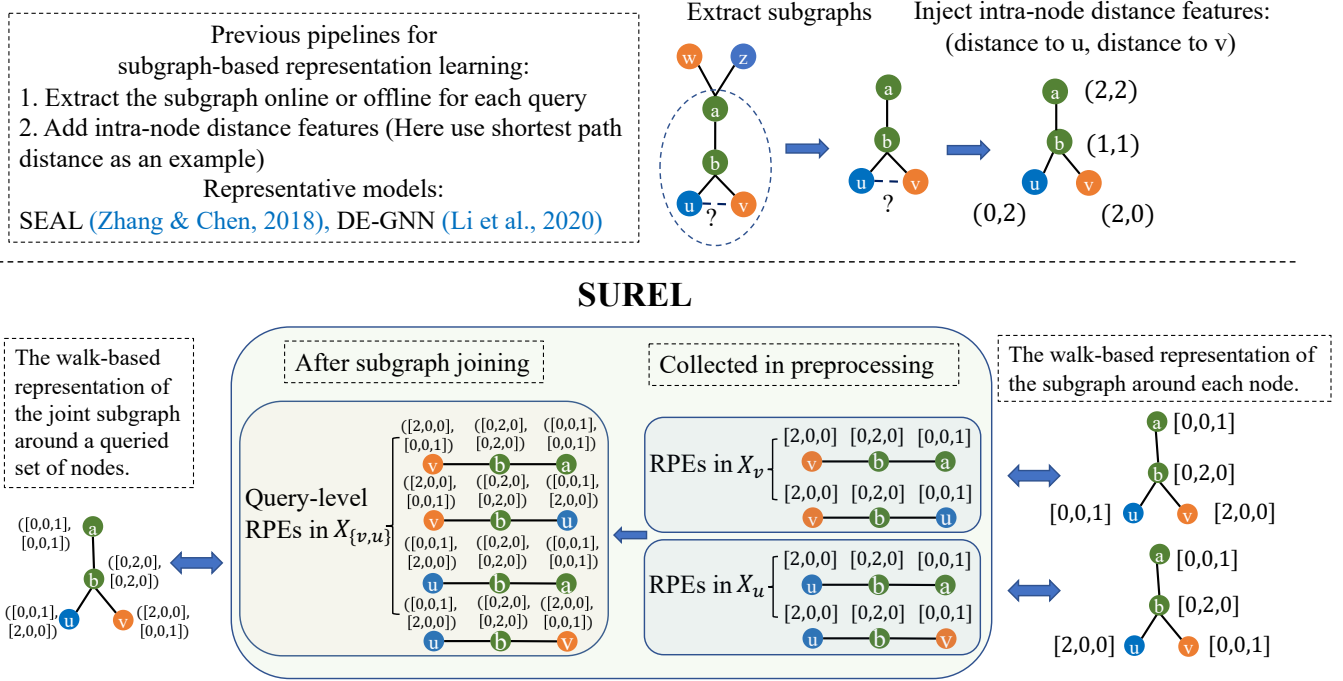


Figure 10: How is SUREL related to previous SGRL models? Previous SGRL models, such as SEAL [54] and DE-GNN [22], first extract the neighboring subgraphs according to the queries and then attach distance features to the nodes. In SUREL, all the subgraphs are represented by sets of walks sampled from the corresponding subgraphs. Given a query, the joint subgraph is represented by the concatenation of sets of walks. The query-level relative positional encoding (RPEs) obtained by joining node-level RPEs that represent the intra-node distance features.

The following parameters are used for the training of SUREL on all tasks mentioned above unless specified otherwise: initial learning rate $1r=1e-3$ with early stopping of 5-epoch patience, dropout $p=0.1$, Adam as the default optimizer, batch capacity $B_1 = 1500$, and batch size $B_2 = 32$ (16 for ppa).

The results reported in Table 3 are obtained through the combination of hyperparameters listed in Table 8. For the profiling of SUREL in Table 5 and Fig. 4, we use the following combinations: citation2 with $m = 50$, $M = 4$, $k = 20$; collab with $m = 2$, $M = 200$, $k = 20$, as relative small values of m , M , k already guarantee sufficient good performance. The rest remains the same as reported earlier.

C.4 Computation Complexity Analysis

We analyze the computation cost in the proposed framework SUREL and identify three major parts:

Random Walks: the space complexity is $O(mM|\mathcal{V}|)$, where $|\mathcal{V}|$ denotes the size of node set of the input graph; the time complexity is $O(mM|\mathcal{V}|/P)$, where P is the number of threads. Practically, the number of steps m generally lies in the range of $2 \sim 5$.

Relative Positional Encoding: the space complexity for RPE is $O(m^2M|\mathcal{V}|)$ as there are at most $m \cdot M$ many distinct nodes in the set of walks originated from a single node. Meanwhile, the space requirement can be further reduced to $1/10$ after pruning and remapping RPE via RPE-ID. RPE can be computed with walk

Table 8: Hyperparameters Used for Benchmarking SUREL.

Dataset	#steps m	#walks M	#neg samples k
citation2	4	200	50
collab	2	400	50
ppa	4	200	50
BALBc1	2	400	-
MAG (P-A)	3	200	10
MAG (P-P)	4	100	50
tags-math	3	100	10
DBLP-coauthor	3	100	10

sampling concurrently. Thus, combining with random walks, the time complexity is still $O(mM|\mathcal{V}|/P)$.

Subgraph Joining: for a query Q , the time complexity is $O(c \cdot mM|Q|/P)$ for joining all associated set of walks in the subgraph. c is a scalar related to the size of Q . In practice, $|Q| = 2$ for link prediction, $|Q| \geq 3$ for higher-order pattern prediction.

C.5 Implementation Details

We implemented our framework on top of PyTorch, NumPy, and OpenMP. uhash is adopted to serve light and high efficient indexing

for RPEs associated with sampled walks. For better parallelization, the computation intensive part is written by C language with bindings to support Python APIs, including walk sampler, RPE encoder, and subgraph joining operation. To reduce the overhead of mixing programming, we use the indices of RPE and the native C/Numpy arrays instead of Python object arrays to exchange results between

function calls and underlying C code. We also provide Python APIs to support customizing above-mentioned operations in parallel. The SUREL framework is open-source at <https://github.com/GraphCOM/SUREL> and free for academic use. The dataset for relation and higher-order pattern prediction is accessible via Box at <https://app.box.com/s/sfmv2k5ow28g8c92bh2b3kzl9ka3vt8l>.